Mathematical Biosciences and Engineering

MBE, 20(8): 14026–14045.
DOI: 10.3934/mbe.2023626
Received: 31 March 2023
Revised: 28 May 2023
Accepted: 16 June 2023
Published: 25 June 2023

http://www.aimspress.com/journal/MBE

Theory article

Design and stabilization analysis of luxury cruise with dynamic positioning systems based on sampled-data control

Zhe Zou[1] and Minjie Zheng[2,*]

[1] Arts and Design College, Jimei University, Jimei, Xiamen 361021, China
[2] Navigation College, Jimei University, Jimei, Xiamen 361021, China

* **Correspondence:** Email: jimi_1205@163.com.

Abstract: This paper studies the sampled-data control issue for a luxury cruise (LC) with dynamic positioning system (DPS). The design method and mathematical model of LC is given. By constructing an improved time-dependent Lyapunov-Krasovskii function (LKF) by adding new useful terms, the sampling pattern is fully captured and less conservatism of the results are obtained. Based on the constructed the LKF, the new stability criterion is obtained and the sampled-data controller for LC with DPS is designed. Finally, an example is exhibited to prove that the proposed approach is valid and applicable.

Keywords: luxury cruise; dynamic positioning system; sampled-data control; Lyapunov-Krasovskii functional; linear matrix inequality

1. Introduction

Dynamic positioning system (DPS) is a system that can automatically control the position and course of a ship [1]. It only depends on its own propulsion system. The position and course of the ship's motion are measured by various sensors equipped by the ship itself, and the computer is used to control the ship's thrust device to generate propulsion force and torque to resist the interference force caused by the external environment. Then the ship can maintain the target's positions and heading. The DPS can fix the ship in a certain position, and can also automatically adjust the heading of the ship to the optimal desired position according to the real-time direction of wind, wave and current. Additionally, it has been widely used in marine investigation ship, drilling ship, salvage ship, mining ship, cable laying ship and so on. By far, severable important control methods have been reported for DPS ([2–7]). Liang et al. [2] studies the state space model of DPS by using Cummins equation and convolution integral term. Based on this model, a static output feedback controller based on L_∞ is designed. Based neural fuzzy algorithm, Fang and Lee [3] use a self-tuning controller to control the rotation speed of the outboard thruster to achieve the goal of controlling the ship's position, heading and path tracking. In Zhang et al. [4], a robust neural control algorithm for DPS based on the combination of dynamic surface control, neural network and robust damping technology is proposed. This algorithm solves the strong coupling between state variables and the uncertainty of actuator gain, reduces the parameter requirements of the DP model. In Ngongi et al. [5], a robust fuzzy controller using optimal control technology is proposed. The controller uses T-S fuzzy model to estimate the nonlinear part of DPS, and uses the generalized eigenvalue method to solve the controller gain. To deal with the issue of the model uncertainties, Li et al. [6] investigated a new collaborative design for path tracking of hybrid USVs and UAVs in the presence of structural uncertainty and external disturbances. In order to control the convergence of USV-UAV to the desired path, an adaptive fuzzy control algorithm was designed by integrating DSC and backstepping technology. In Zhang et al. [7], by combining robust neural damping with DSC technology, the gain dependent adaptive laws for the ships have been developed to address constraints of gain uncertainty and environmental disturbances.

Due to the wide application of digital circuits, microelectronic devices and modern computers, the sampled-data system has developed rapidly. The sampled-data control system is a kind of hybrid system, which combines the characteristics of discrete system and continuous system. Therefore, it can effectively reduce the consumption of computing resources, reduce the burden of communication transmission and is easier to implement in engineering. Recently, the sampled-data control theory has become one of the research hotspots in multiagent systems [8,9], fuzzy systems [10–12], chaotic systems [13–15], neural networks systems [16–18] and so on ([19–24]), and has wide applications in train systems [25], airship systems [26] and ship systems [27]. Scholars have made corresponding achievements in sampled-data control ([28–33]). Qian et al. [29] discussed the global stabilization of a class of nonlinear systems with higher order powers based on output feedback sampling control. A linear output feedback sampled-data controller is constructed in Zhang et al. [30], which can semi globally asymptotically stabilize the system with high order and linear growth nonlinearity. Zou et al. [31] designed a sampling control protocol using the backstep-ping method to ensure the leader follower consistency of second-order multi-agent with external interference and unpredictable speed information. In Zhang et al. [32], the global output feedback decentralized control problem for a class of uncertain interconnected systems based on sampled-data control is studied. By constructing sampled high gain observers and controllers, the corresponding system is guaranteed to be globally asymptotically stable.

DPS is a system controller by computer. Recently, sampled-data theory has been used to solve the control issue of DPS. In Katayama [34], the nonlinear sampled-data control issue of DPS is discussed by using the integrator backstepping technique and a semiglobal stability controller is designed. In Katayama and Aoki [35], the linear trajectory tracking issue for sampled-data DPS is discussed. Additionally, a state-feedback controller and observer are designed based on the Euler approximation model. In Zheng et al. [36], robust sampled-data control of neutral system for DPS is discussed. the state-derivative control law is designed. By combining the delayed decomposition technique and Wirtinger based integral inequality, less conservative results are obtained. In Yang and Zheng [37], the fault-tolerant control for sampled-data DPS with actuator failures is discussed. Zheng et al. [38]

discusses the nonlinear fuzzy sampled-data control issue for DPS, and a free weighting matrix is used to ensure the stability of the system. In Chen et al. [39], the tracking control of DPS with actuator-failure and aperiodic measurement information is studied. Additionally, aperiodic sampling data controller is designed to guarantee that the DPS has excellent tracking performance.

Although some researches have been reported on the sampled-data control DPS, there is still much room for improvement. One reason is that the term in LKF share common quadratic function, which may lead to conservative result. The other reason is that due to the neglect of some important and useful terms in LKF, the available features of the actual sampling mode are not fully captured, which may lead to conservatism to a certain extent.

Motivated by the discussion, the design and stabilization of sampled-data for LC with DPS is discussed in this paper. First, the design method for LC is given. Second, the motion model of LC with DPS is established. Third, a novel LKF is introduced to capture the sampling pattern fully. Then, the stability conditions of the system are derived by LMIs and corresponding design algorithm of the controller is given. Finally, a specific example verifies the effectiveness of the proposed method.

2. Design of luxury cruise

To solve the current problem such as ship function, aesthetic and humanization, we should base on the related theories of product system design and integrate design art and ship engineering knowledge in a scientific, systematic way to obtain the method of ship design innovation.

Due to the highly humanization, highly esthetic, highly functional and highly technology-integrated characteristics, it is of typical significance that we take cruise ship as representatives to do research and for educational means.

Then, a 150 m five-star luxury cruise is designed as follow. Figure 1 shows the three-dimensional modelling, Figure 2 is the panoramic effect picture and Figure 3 is nightscape effect picture of the luxury cruise.

Figure 1. Three-dimensional modelling of luxury cruise.

Figure 2. Panoramic effect picture of luxury cruise.

Figure 3. Nightscape effect picture of luxury cruise.

3. Problem formulation

This article focuses on the fixed point control of ships on the sea surface, so the influence on heave, sway and pitch is ignored, and only the three degrees of freedom of heave, sway and yaw which have significant effects on ship are considered. Hence, the following mathematical model of the LC with DPS is considered.

$$\begin{aligned} &\boldsymbol{M}\dot{\upsilon}(t)+\boldsymbol{D}\upsilon(t)=u(t)+w(t),\\ &\dot{\boldsymbol{\eta}}(t)=\boldsymbol{J}\left(\psi(t)\right)\boldsymbol{\upsilon}(t), \end{aligned} \tag{1}$$

where

$$\boldsymbol{M}=\begin{bmatrix} m-X_{\dot{u}} & 0 & 0 \\ 0 & m-Y_{\dot{v}} & mx_G-Y_{\dot{r}} \\ 0 & mx_G-Y_{\dot{r}} & I_z-N_{\dot{r}} \end{bmatrix}, \boldsymbol{D}=\begin{bmatrix} -X_u & 0 & 0 \\ 0 & -Y_v & -Y_r \\ 0 & -N_v & -N_r \end{bmatrix},$$
$$\boldsymbol{J}\left(\psi(t)\right)=\begin{bmatrix} \cos\left(\psi(t)\right) & -\sin\left(\psi(t)\right) & 0 \\ \sin\left(\psi(t)\right) & \cos\left(\psi(t)\right) & 0 \\ 0 & 0 & 1 \end{bmatrix}.$$

where $\boldsymbol{\eta}(t)=\left[x_a(t) \quad y_a(t) \quad \psi(t)\right]^T$ shows the position and heading angle of the ship in the northeast coordinate system, $\boldsymbol{\upsilon}(t)=\left[p(t) \quad v(t) \quad r(t)\right]^T$ describes the speed and heading rotation rate of the ship in the hull coordinate system (see Figure 4). $\boldsymbol{J}(\psi)$ is the rotation matrix, $u(t)=\left[u_1(t),u_2(t),u_3(t)\right]$ are the control force vectors provided by the thruster, where $u_1(t)$ is the forward control force, $u_2(t)$ is the lateral drift control force, and $u_3(t)$ is the yaw control torque. M is the inertial matrix, and D is damping matrix. m is the ship's mass, and I_z is the rotational inertia; X_u, Y_v, N_r are the linear damping coefficients of the ship in three degrees of freedom, and $X_{\dot{u}}, Y_{\dot{v}}, N_{\dot{r}}$ are the additional mass generated by the ship in the surge, sway and yaw. $w(t)=\left[w_1(t),w_2(t),w_3(t)\right]$ is an unknown disturbance term that represents the environmental disturbances such as wind, waves and currents.

Assume that the environment disturbance is unknown but energy bounded, that is, $|w_i(t)|\le h$, h is upper bound of the disturbances.

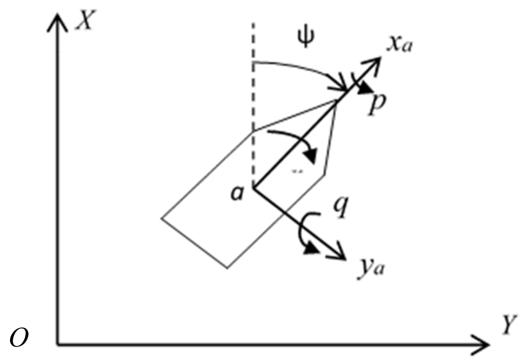

Figure 4. Body-fixed coordinate systems.

Assume that yaw angle $\psi(t)$ is small enough, which means that $\cos(\psi(t)) \approx 1, \sin(\psi(t)) \approx 0$, then

$$J(\psi(t)) \approx I. \tag{2}$$

Define

$$x(t) = \begin{bmatrix} \eta(t) & \upsilon(t) \end{bmatrix}^T = \begin{bmatrix} x_p(t) & y_p(t) & \psi(t) & p(t) & q(t) & r(t) \end{bmatrix}^T \tag{3}$$

Substitute (3) into (1) that

$$\dot{x}(t) = \boldsymbol{A}x(t) + \boldsymbol{B}u(t) + \boldsymbol{B}_w w(t), \tag{4}$$

where

$$\boldsymbol{A} = \begin{bmatrix} 0_{3\times3} & I_{3\times3} \\ 0_{3\times3} & -M^{-1}D \end{bmatrix}, \quad \boldsymbol{B} = \begin{bmatrix} 0_{3\times3} \\ M^{-1} \end{bmatrix}, \quad \boldsymbol{B}_w = \begin{bmatrix} 0_{3\times3} \\ M^{-1} \end{bmatrix}.$$

Assume that the state variable of the DPS is sampled by the time $0 = t_0 < t_1 < \cdots < t_k < \cdots < \lim_{k\to\infty} t_k = +\infty$. Assume the sampling period is

$$t_{k+1} - t_k \le d, \forall k \ge 0, d > 0,$$

where d is the upper bound of the sampling period. The sampled-data controller is designed

$$u(t) = \boldsymbol{K}x(t_k), \quad t_k \le t < t_{k+1}, \tag{5}$$

where $\boldsymbol{K}$ is controller gain matrix.

Substitute (5) into (4), it can be obtained

$$\dot{x}(t) = \boldsymbol{A}x(t) + \boldsymbol{BK}x(t_k) + \boldsymbol{B}_w x(t) \tag{6}$$

The paper's aim is to propose a sampled-data controller to guarantee the stability of the system. To derive our main theorems, the following lemma is introduced.

Lemma 1([40]): For scalars $\tau_2 > \tau_1$, any constant matrix $\boldsymbol{Z} \in R^n, \boldsymbol{Z} > 0$, vector function $w : [\tau_1, \tau_2] \in R^n$, the following inequalities are established

$$-\int_{t-\tau_2}^{t-\tau_1} w^T(\alpha) Z w(\alpha) d\alpha \le -\frac{1}{\tau_2 - \tau_1} \left(\int_{t-\tau_2}^{t-\tau_1} w^T(\alpha) d\alpha \right)^T \boldsymbol{Z} \left(\int_{t-\tau_2}^{t-\tau_1} w(\alpha) d\alpha \right) \tag{7}$$

$$-\int_{-\tau_2}^{-\tau_1} \int_{t+\alpha}^{t} w^T(s) Z w(s) ds d\alpha \le -\frac{2}{\tau_2^2 - \tau_1^2} \left(\int_{-\tau_2}^{-\tau_1} \int_{t+\alpha}^{t} w^T(s) ds d\alpha \right)^T \boldsymbol{Z} \left(\int_{-\tau_2}^{-\tau_1} \int_{t+\alpha}^{t} w(s) ds d\alpha \right) \tag{8}$$

4. Main results

In the section, the stability conditions for system (6) are proposed. Consequently, a sampled-data controller is developed. First, the notations are defined as follow:

$$\begin{aligned}
&\tau(t) = t - t_k,\ d(t) = d - \tau(t), \\
&\varsigma(t) = \begin{bmatrix} x^T(t) & x^T(t_k) & \int_{t_k}^{t} x^T(s) ds \end{bmatrix}^T \\
&\zeta(t) = \begin{bmatrix} x^T(t) & \dot{x}(t)^T & x^T(t_k) & \int_{t_k}^{t} x^T(s) ds \end{bmatrix}
\end{aligned}$$

Theorem 1: The system (6) with $w(t) = 0$ is asymptotically stable, if there exist symmetric positive matrices $\boldsymbol{P} > 0, \boldsymbol{Q} > 0, \boldsymbol{Z} > 0, \boldsymbol{R} > 0, \boldsymbol{U} > 0,\quad \boldsymbol{X}_{11}, \boldsymbol{X}_{13}, \boldsymbol{X}_{22}, \boldsymbol{X}_{23}, \boldsymbol{X}_{33}, \boldsymbol{G}, \boldsymbol{M}_i, \boldsymbol{N}_i\ (i = 1,2,3,4)$ and scales $d > 0, \varepsilon_i\ (i = 1,2,3,4)$, such that the following LMIs hold:

$$\Psi_1 = \begin{bmatrix} \boldsymbol{P} + d\left(\boldsymbol{X}_{11} + \boldsymbol{X}_{11}^T + \boldsymbol{Q}\right) & d\left(\boldsymbol{X}_{11} + \boldsymbol{X}_{22} - \boldsymbol{Q}\right) & d\boldsymbol{X}_{13} \\ * & d\left(\boldsymbol{X}_{11} + \boldsymbol{X}_{22}^T + \boldsymbol{Q}\right) & d\boldsymbol{X}_{23} \\ * & * & d\boldsymbol{X}_{33} \end{bmatrix} > 0 \tag{9}$$

$$\Psi_2 = \begin{bmatrix} \Xi_{11} + \Omega_{11} & \Xi_{12} + \Omega_{12} & \Xi_{13} + \Omega_{13} & \Xi_{14} + d\boldsymbol{X}_{33}^T \\ * & \Xi_{22} + \Omega_{22} & \Xi_{23} + \Omega_{23} & \Xi_{24} + d\boldsymbol{X}_{13} \\ * & * & \Xi_{33} + \Omega_{33} & \Xi_{34} \\ * & * & * & \Xi_{44} \end{bmatrix} < 0 \tag{10}$$

$$\Psi_3 == \begin{bmatrix} \Pi_{11} & \Pi_{12} \\ * & \Pi_{22} \end{bmatrix} < 0. \tag{11}$$

where

$$\Pi_{11} = \begin{bmatrix} \Xi_{11} + \Omega_{11} & \Xi_{12} + d\boldsymbol{N}_2^T & \Xi_{13} + d\boldsymbol{N}_3^T & \Xi_{14} + d\boldsymbol{N}_4^T \\ * & \Xi_{22} + \frac{d^2}{4}\boldsymbol{Z} & \Xi_{23} & \Xi_{24} \\ * & * & \Xi_{33} + \Omega_{33} & \Xi_{34} \\ * & * & * & \Xi_{44} \end{bmatrix},$$

$$\Pi_{12} = \begin{bmatrix} -d\boldsymbol{M}_1 & d\boldsymbol{N}_1 \\ -d\boldsymbol{M}_2 & d\boldsymbol{N}_2 \\ -d\boldsymbol{R}_{12}^T - d\boldsymbol{M}_3 & d\boldsymbol{N}_3 \\ -d\boldsymbol{M}_4 & d\boldsymbol{N}_4 \end{bmatrix},$$

$$\Pi_{22} = \begin{bmatrix} -d\boldsymbol{Q} - d\boldsymbol{R}_{11} & 0 \\ * & -2\boldsymbol{Z} \end{bmatrix},$$

$$\Xi_{11} = -\left(\boldsymbol{X}_{11} + \boldsymbol{X}_{11}^T\right) + \boldsymbol{M}_1^T + \boldsymbol{M}_1 + \varepsilon_1 \boldsymbol{A}\boldsymbol{G}^T + \varepsilon_1 \boldsymbol{G}\boldsymbol{A}^T$$

$$\Xi_{12} = \boldsymbol{P} + \boldsymbol{M}_2^T - \varepsilon_1 \boldsymbol{G} - \varepsilon_2 \boldsymbol{A}^T\boldsymbol{G}^T$$

$$\Xi_{13} = \left(\boldsymbol{X}_{11} + \boldsymbol{X}_{22}\right) + \boldsymbol{M}_3^T - \boldsymbol{M}_1 + \varepsilon_1 \boldsymbol{G}\boldsymbol{B}\boldsymbol{K} + \varepsilon_3 \boldsymbol{A}^T\boldsymbol{G}^T$$

$$\Xi_{14} = -\boldsymbol{X}_{13} + \boldsymbol{M}_4^T - \boldsymbol{N}_1 + \varepsilon_4 \boldsymbol{A}^T\boldsymbol{G}^T$$

$$\Xi_{22} = -\varepsilon_2 \boldsymbol{G} - \varepsilon_2 \boldsymbol{G}^T$$

$$\Xi_{23} = -\boldsymbol{M}_2 + \varepsilon_2 \boldsymbol{G}\boldsymbol{B}\boldsymbol{K} - \varepsilon_3 \boldsymbol{G}^T$$

$$\Xi_{24} = -\varepsilon_4 \boldsymbol{G}^T - \boldsymbol{N}_2$$

$$\Xi_{33} = -\left(\boldsymbol{X}_{22} + \boldsymbol{X}_{22}^T\right) - \boldsymbol{M}_3^T - \boldsymbol{M}_3 + \varepsilon_3 \boldsymbol{G}\boldsymbol{B}\boldsymbol{K} + \varepsilon_3 \boldsymbol{K}^T\boldsymbol{B}^T\boldsymbol{G}^T$$

$$\Xi_{34} = -\boldsymbol{X}_{23} - \boldsymbol{U}_{12} - \boldsymbol{M}_4^T - \boldsymbol{N}_3 + \varepsilon_4 \boldsymbol{K}^T\boldsymbol{B}^T\boldsymbol{G}^T$$

$$\Xi_{44} = -\boldsymbol{X}_{33} - \frac{1}{d}\boldsymbol{U}_{22} - \boldsymbol{N}_4^T - \boldsymbol{N}_4$$

$$\Omega_{11} = d\left(\boldsymbol{X}_{13} + \boldsymbol{X}_{13}^T\right) + d\boldsymbol{U}_{22} - \boldsymbol{Z}$$

$$\Omega_{12} = d\boldsymbol{X}_{11} + d\boldsymbol{X}_{11}^T$$

$$\Omega_{13} = d\boldsymbol{X}_{23}^T + d\boldsymbol{U}_{12}^T + \boldsymbol{Z}$$

$$\Omega_{22} = d\boldsymbol{R}_{11} + d\boldsymbol{Q} + \frac{d^2}{4}\boldsymbol{Z}$$

$$\Omega_{23} = -d\left(\boldsymbol{X}_{11} + \boldsymbol{X}_{22}\right) + d\boldsymbol{R}_{12}$$

$$\Omega_{33} = d\boldsymbol{R}_{22} + d\boldsymbol{U}_{11} - \boldsymbol{Z}.$$

Proof. Consider the following LKF

$$V(t)=\sum_{i=1}^{4}V_i(t), \quad t\in[t_k,t_{k+1}) \tag{12}$$

$$\begin{aligned}
V_1(t) &= x(t)^T \boldsymbol{P}x(t)+d(t)\varsigma(t)^T \boldsymbol{X}\varsigma(t)+d(t)\int_{t_k}^{t}\dot{x}(s)^T \boldsymbol{Q}\dot{x}(s)ds\\
V_2(t) &= d(t)\int_{t_k}^{t}\begin{bmatrix}\dot{x}(s)\\ x(t_k)\end{bmatrix}^T \boldsymbol{R}\begin{bmatrix}\dot{x}(s)\\ x(t_k)\end{bmatrix}ds\\
V_3(t) &= d(t)\int_{t_k}^{t}\begin{bmatrix}x(t_k)\\ x(s)\end{bmatrix}^T \boldsymbol{U}\begin{bmatrix}x(t_k)\\ x(s)\end{bmatrix}ds\\
V_4(t) &= d(t)\int_{-d(t)}^{0}\int_{t+\theta}^{t}\dot{x}(s)^T \boldsymbol{Z}\dot{x}(s)dsd\theta
\end{aligned}$$

where

$$\boldsymbol{X}=\begin{bmatrix}\boldsymbol{X}_{11}+\boldsymbol{X}_{11}^T & -\boldsymbol{X}_{11}-\boldsymbol{X}_{22} & \boldsymbol{X}_{13}\\ * & \boldsymbol{X}_{22}+\boldsymbol{X}_{22}^T & \boldsymbol{X}_{23}\\ * & * & \boldsymbol{X}_{33}\end{bmatrix},\boldsymbol{R}=\begin{bmatrix}\boldsymbol{R}_{11} & \boldsymbol{R}_{12}\\ * & \boldsymbol{R}_{22}\end{bmatrix},\boldsymbol{U}=\begin{bmatrix}\boldsymbol{U}_{11} & \boldsymbol{U}_{12}\\ * & \boldsymbol{U}_{22}\end{bmatrix}$$

By Lemma 1, it can be verified that

$$\begin{aligned}
V_1(t) &\geq x(t)^T \boldsymbol{P}x(t)+d(t)\varsigma(t)^T \boldsymbol{X}\varsigma(t)+\frac{d(t)}{d}\left[x(t)-x(t_k)\right]^T \boldsymbol{Q}\left[x(t)-x(t_k)\right]\\
&=\frac{d(t)}{d}\varsigma^T(t)\Psi_1^{ij}\varsigma(t)
\end{aligned} \tag{13}$$

From LMI (9), $V_1(t)\geq 0$ can be concluded, which means that $V(t)\geq 0$.
Calculate the derivative of $V(t)$, it yields that

$$\begin{aligned}
\dot{V}_1(t) &= 2\dot{x}(t)^T \boldsymbol{P}x(t)+2d(t)\varsigma^T(t)\boldsymbol{X}\begin{bmatrix}\dot{x}^T(t) & 0 & x^T(t)\end{bmatrix}^T\\
&\quad -\varsigma^T(t)\boldsymbol{X}\varsigma(t)+d(t)\dot{x}^T(t)\boldsymbol{Q}\dot{x}(t)-\int_{t_k}^{t}\dot{x}^T(s)\boldsymbol{Q}\dot{x}(s)ds,\\
\dot{V}_2(t) &= d(t)\begin{bmatrix}\dot{x}(t)\\ x(t_k)\end{bmatrix}^T \boldsymbol{R}\begin{bmatrix}\dot{x}(t)\\ x(t_k)\end{bmatrix}-\int_{k}^{t}\begin{bmatrix}\dot{x}(s)\\ x(t_k)\end{bmatrix}^T \boldsymbol{R}\begin{bmatrix}\dot{x}(s)\\ x(t_k)\end{bmatrix}ds,\\
\dot{V}_3(t) &= d(t)\begin{bmatrix}x(t_k)\\ x(t)\end{bmatrix}^T \boldsymbol{U}\begin{bmatrix}x(t_k)\\ x(t)\end{bmatrix}-\int_{t_k}^{t}\begin{bmatrix}x(t_k)\\ x(s)\end{bmatrix}^T \boldsymbol{U}\begin{bmatrix}x(t_k)\\ x(s)\end{bmatrix}ds\\
&= d(t)\begin{bmatrix}x(t_k)\\ x(t)\end{bmatrix}^T \boldsymbol{U}\begin{bmatrix}x(t_k)\\ x(t)\end{bmatrix}-\tau(t)x^T(t_k)\boldsymbol{U}_{11}x(t_k)\\
&= -2x^T(t_k)\boldsymbol{U}_{12}\int_{t_k}^{t}x(s)ds-\int_{t_k}^{t}x^T(s)\boldsymbol{U}_{22}x(s)ds
\end{aligned}$$

$$
\begin{aligned}
\dot{V}_4(t) &= d(t)\tau(t)\dot{x}^T(t)\boldsymbol{Z}\dot{x}(t) - d(t)\int_{t_k}^{t}\dot{x}^T(s)\boldsymbol{Z}\dot{x}(s)ds - \int_{-\tau(t)}^{0}\int_{t+\alpha}^{t}\dot{x}^T(s)\boldsymbol{Z}\dot{x}(s)dsd\alpha \\
&\le \frac{\left(d(t)+\tau(t)\right)^2}{4}\dot{x}^T(t)\boldsymbol{Z}\dot{x}(t) - d(t)\int_{t_k}^{t}\dot{x}^T(s)\boldsymbol{Z}\dot{x}(s)ds - \int_{-\tau(t)}^{0}\int_{t+\alpha}^{t}\dot{x}^T(s)\boldsymbol{Z}\dot{x}(s)dsd\alpha \\
&\le \frac{d}{4}d(t)\dot{x}^T(t)\boldsymbol{Z}\dot{x}(t) + \frac{d}{4}\tau(t)\dot{x}^T(t)\boldsymbol{Z}\dot{x}(t) - \frac{d(t)}{d}\begin{bmatrix} x(t_k) \\ x(t) \end{bmatrix}^T \begin{bmatrix} \boldsymbol{Z} & -\boldsymbol{Z} \\ -\boldsymbol{Z} & \boldsymbol{Z} \end{bmatrix}\begin{bmatrix} x(t_k) \\ x(t) \end{bmatrix} \\
&\quad - \int_{-\tau(t)}^{0}\int_{t+\alpha}^{t}\dot{x}^T(s)\boldsymbol{Z}\dot{x}(s)dsd\alpha
\end{aligned} \tag{14}
$$

By Lemma 1, one can obtain

$$
\begin{aligned}
0 &= 2\xi^T(t)\boldsymbol{N}\times[\tau(t)x(t) - \int_{t_k}^{t}x(s)ds - \int_{-\tau(t)}^{0}\int_{t+\alpha}^{t}\dot{x}(s)dsd\alpha] \\
&\le 2\tau(t)\xi^T(t)\boldsymbol{N}x(t) - 2\xi^T(t)\boldsymbol{N}\int_{t_k}^{t}x(s)ds + \frac{\tau^2(t)}{2}\xi^T(t)\boldsymbol{N}Z^{-1}N^T\xi(t) \\
&\quad + \frac{2}{\tau^2(t)}\left[\int_{-\tau(t)}^{0}\int_{t+\alpha}^{t}\dot{x}^T(s)dsd\alpha\right]\boldsymbol{Z}\left[\int_{-\tau(t)}^{0}\int_{t+\alpha}^{t}\dot{x}(s)dsd\alpha\right] \\
&\le 2\tau(t)\xi^T(t)\boldsymbol{N}x(t) - 2\xi^T(t)\boldsymbol{N}\int_{t_k}^{t}x(s)ds + \frac{\tau^2(t)}{2}\xi^T(t)\boldsymbol{N}\boldsymbol{Z}^{-1}\boldsymbol{N}^T\xi(t) + \int_{-\tau(t)}^{0}\int_{t+\alpha}^{t}\dot{x}^T(s)\boldsymbol{Z}\dot{x}(s)dsd\alpha
\end{aligned} \tag{15}
$$

which implies

$$
\int_{-\tau(t)}^{0}\int_{t+\alpha}^{t}\dot{x}(s)Z\dot{x}(s)dsd\alpha \le 2\tau(t)\xi^T(t)Nx(t) - 2\xi^T(t)N\int_{t_k}^{t}x(s)ds + \frac{d\tau(t)}{2}\xi^T(t)NZ^{-1}N^T\xi(t) \tag{16}
$$

Combining (14) with (16) that

$$
\begin{aligned}
\dot{V}_4(t) &\le \frac{d}{4}d(t)\dot{x}^T(t)\boldsymbol{Z}\dot{x}(t) + \frac{d}{4}\tau(t)\dot{x}^T(t)\boldsymbol{Z}\dot{x}(t) - \frac{d(t)}{d}\begin{bmatrix} x(t_k) \\ x(t) \end{bmatrix}^T \begin{bmatrix} \boldsymbol{Z} & -\boldsymbol{Z} \\ -\boldsymbol{Z} & \boldsymbol{Z} \end{bmatrix}\begin{bmatrix} x(t_k) \\ x(t) \end{bmatrix} \\
&\quad + 2\tau(t)\xi^T(t)\boldsymbol{N}x(t) - 2\xi^T(t)\boldsymbol{N}\int_{t_k}^{t}x(s)ds + \frac{d\tau(t)}{2}\xi^T(t)\boldsymbol{N}\boldsymbol{Z}^{-1}\boldsymbol{N}^T\xi(t)
\end{aligned} \tag{17}
$$

For any matrixes $\boldsymbol{G}$, $\boldsymbol{M}$, and scalars $\varepsilon_i, i = 1,2,3,4$, we have

$$
0 = \xi^T(t)\boldsymbol{M}\times\left[x(t) - x(t_k) - \int_{t_k}^{t}\dot{x}(s)ds\right] \tag{18}
$$

$$
0 = 2\left[\varepsilon_1 x^T(t)\boldsymbol{G} + \varepsilon_2\dot{x}^T(t)\boldsymbol{G} + \varepsilon_3 x(t_k)\boldsymbol{G} + \varepsilon_4\int_{t_k}^{t}x^T(s)\boldsymbol{G}ds\right]\times\left[-\dot{x}(t) + \boldsymbol{A}x(t) + \boldsymbol{B}\boldsymbol{K}x(t_k)\right] \tag{19}
$$

From (13),(14) and (17)–(19), we obtain that

$$
\dot{V}(t) \le \frac{d(t)}{d}\xi^T(t)\Psi_3\xi(t) + \frac{1}{d}\int_{t_k}^{t}\begin{bmatrix} \xi(t) \\ \dot{x}(s) \end{bmatrix}^T \hat{\Psi}_4 \begin{bmatrix} \xi(t) \\ \dot{x}(s) \end{bmatrix} ds \tag{20}
$$

where

$$\hat{\Psi}_4 = \begin{bmatrix} \Pi_{11} & \Theta \\ * & -d\boldsymbol{Q} - \boldsymbol{R}_{11} \end{bmatrix} + \frac{d^2}{2} \begin{bmatrix} \boldsymbol{N} \\ 0 \end{bmatrix} \boldsymbol{Z}^{-1} \begin{bmatrix} \boldsymbol{N} \\ 0 \end{bmatrix}^T$$
$$\Theta_{ij} = \begin{bmatrix} -d\boldsymbol{M}_1^T & -d\boldsymbol{M}_2^T & -d\boldsymbol{R}_{12} - d\boldsymbol{M}_3^T & -d\boldsymbol{M}_4^T \end{bmatrix}^T \tag{21}$$

Following the Schur complement, (21) implies $\hat{\Psi}_4^{ij} < 0$. which implies that $\dot{V}(t) < -\sigma \|x(t)\|^2$ when $x(t) \neq 0, \sigma > 0$. Thus, the system (6) is asymptotically stable. This completed the proof.

Remark 1: Note that some novel terms such as $d(t)\int_{-d(t)}^{0}\int_{t+\theta}^{t} \dot{x}(s)^T Z\dot{x}(s)dsd\theta$ are added in the constructed LKF, which means that the characteristics about sampling patterns are fully captured.

Remark 2: If $\boldsymbol{Q} = \boldsymbol{R}_{12} = \boldsymbol{R}_{22} = \boldsymbol{Z} = 0$ and $\boldsymbol{X}_{13} = \boldsymbol{X}_{23} = \boldsymbol{X}_{33} = \boldsymbol{U}_{13} = \boldsymbol{U}_{12} = \boldsymbol{U}_{22} = 0$, the LKF is simplified to that in [38] and [39]. Therefore, the proposed LKF are general and have wider application scopes. Moreover, according to Newton-Leibniz formulas, free matrices M and N have been considered to handle the derivation of LKF to avoid using the bounding techniques. Therefore, the conservatism is reduced.

Remark 3: Compared with [38] and [39], the more relaxed constraint conditions are introduced by adding X-dependent term in $V_1(t)$, which means that the involved symmetric matrices are not required to be positive definite. Besides, the term $d(t)\int_{t_k}^{t} \dot{x}^T(s)\boldsymbol{Q}\dot{x}(s)ds$ is added in the LKF to obtain more relaxed condition and longer sampling period. Hence, the conservativeness can be further reduced.

Remark 4: The number of decision variables in the paper is $12n^2 + 13n$, which depends on the system order n. When n increase, it will consume longer central processing unit time when solving stability conditions. Furthermore, it is worth noting that the number of decision variables in [41] and [42] is $70n^2 + 12n$ and $142n^2 + 18n$, which is bigger than that in the paper. This means that the solution of the condition in [41] and [42] will waste more time to obtain less conservative results. It illustrates that the proposed methodology has lower computational complexity than [41] and [42].

Furthermore, the controller design algorithm is introduced via the following theorem.

Theorem 2: The system (6) with $w(t) = 0$ is asymptotically stable, if there exist symmetric positive matrices $\tilde{P} > 0, \tilde{Q} > 0, \tilde{Z} > 0, \tilde{R} > 0, \tilde{U} > 0,$ $\tilde{X}_{11}, \tilde{X}_{13}, \tilde{X}_{22}, \tilde{X}_{23}, \tilde{X}_{33}, \tilde{G}, \tilde{M}_i, \tilde{N}_i$ $(i = 1,2,3,4)$ and scales $d > 0, \varepsilon_i$ $(i = 1,2,3,4)$, such that:

$$\Psi_1^{ij} = \begin{bmatrix} \tilde{\boldsymbol{P}} + d\left(\tilde{\boldsymbol{X}}_{11} + \tilde{\boldsymbol{X}}_{11}^T + \tilde{\boldsymbol{Q}}\right) & d\left(\tilde{\boldsymbol{X}}_{11} + \tilde{\boldsymbol{X}}_{22} - \tilde{\boldsymbol{Q}}\right) & d\tilde{\boldsymbol{X}}_{13} \\ * & d\left(\tilde{\boldsymbol{X}}_{11} + \tilde{\boldsymbol{X}}_{22}^T + \tilde{\boldsymbol{Q}}\right) & d\tilde{\boldsymbol{X}}_{23} \\ * & * & d\tilde{\boldsymbol{X}}_{33} \end{bmatrix} > 0 \tag{22}$$

$$\tilde{\Psi}_2 = \begin{bmatrix} \tilde{\Xi}_{11} + \tilde{\Omega}_{11} & \tilde{\Xi}_{12} + \tilde{\Omega}_{12} & \tilde{\Xi}_{13} + \tilde{\Omega}_{13} & \tilde{\Xi}_{14} + d\tilde{\boldsymbol{X}}_{33}^T \\ * & \tilde{\Xi}_{22} + \tilde{\Omega}_{22} & \tilde{\Xi}_{23} + \tilde{\Omega}_{23} & \tilde{\Xi}_{24} + d\tilde{\boldsymbol{X}}_{13} \\ * & * & \tilde{\Xi}_{33} + \tilde{\Omega}_{33} & \tilde{\Xi}_{34} \\ * & * & * & \tilde{\Xi}_{44} \end{bmatrix} < 0 \tag{23}$$

$$\Psi_3 = \begin{bmatrix} \tilde{\Pi}_{11} & \tilde{\Pi}_{12} \\ * & \tilde{\Pi}_{22} \end{bmatrix} < 0, \tag{24}$$

where

$$\tilde{\Pi}_{11} = \begin{bmatrix} \tilde{\Xi}_{11} + \tilde{\Omega}_{11} & \tilde{\Xi}_{12} + d\tilde{\boldsymbol{N}}_2^T & \tilde{\Xi}_{13} + d\tilde{\boldsymbol{N}}_3^T & \tilde{\Xi}_{14} + d\tilde{\boldsymbol{N}}_4^T \\ * & \tilde{\Xi}_{22} + \frac{d^2}{4}\tilde{\boldsymbol{Z}} & \tilde{\Xi}_{23} & \tilde{\Xi}_{24} \\ * & * & \tilde{\Xi}_{33} + \tilde{\Omega}_{33} & \tilde{\Xi}_{34} \\ * & * & * & \tilde{\Xi}_{44} \end{bmatrix},$$

$$\tilde{\Pi}_{12} = \begin{bmatrix} -d\tilde{\boldsymbol{M}}_2 & d\tilde{\boldsymbol{N}}_2 \\ -d\tilde{\boldsymbol{M}}_3 & d\tilde{\boldsymbol{N}}_3 \\ -d\tilde{R}_{12}^T - d\tilde{\boldsymbol{M}}_3 & d\tilde{\boldsymbol{N}}_3 \\ -d\tilde{\boldsymbol{M}}_4 & d\tilde{\boldsymbol{N}}_4 \end{bmatrix},$$

$$\tilde{\Pi}_{22} = \begin{bmatrix} -d\tilde{\boldsymbol{Q}} - d\tilde{\boldsymbol{R}}_{11} & 0 \\ * & -2\tilde{\boldsymbol{Z}} \end{bmatrix}.$$

$$\tilde{\Xi}_{11} = -\tilde{\boldsymbol{X}}_{11} - \tilde{\boldsymbol{X}}_{11}^T + \tilde{\boldsymbol{M}}_1^T + \tilde{\boldsymbol{M}}_1 - \varepsilon_1 \boldsymbol{A}\tilde{\boldsymbol{G}}^T - \varepsilon_1 \tilde{\boldsymbol{G}}\boldsymbol{A}^T$$

$$\tilde{\Xi}_{12} = \tilde{\boldsymbol{P}} + \tilde{\boldsymbol{M}}_2^T + \varepsilon_1 \tilde{\boldsymbol{G}} - \varepsilon_2 \boldsymbol{A}^T \tilde{\boldsymbol{G}}^T$$

$$\tilde{\Xi}_{13} = \tilde{\boldsymbol{X}}_{11} + \tilde{\boldsymbol{X}}_{22} + \tilde{\boldsymbol{M}}_3^T - \tilde{\boldsymbol{M}}_1 - \varepsilon_1 \boldsymbol{B}\tilde{\boldsymbol{K}} - \varepsilon_3 \tilde{\boldsymbol{G}}\boldsymbol{A}^T$$

$$\tilde{\Xi}_{14} = -\tilde{\boldsymbol{X}}_{13} + \tilde{\boldsymbol{M}}_4^T - \tilde{\boldsymbol{N}}_1 - \varepsilon_4 \tilde{\boldsymbol{G}}\boldsymbol{A}^T$$

$$\tilde{\Xi}_{22} = \varepsilon_2 \tilde{\boldsymbol{G}} + \varepsilon_2 \tilde{\boldsymbol{G}}^T$$

$$\tilde{\Xi}_{23} = -\tilde{\boldsymbol{M}}_2 - \boldsymbol{B}\tilde{\boldsymbol{K}} + \varepsilon_3 \tilde{\boldsymbol{G}}$$

$$\tilde{\Xi}_{24} = \varepsilon_4 \tilde{\boldsymbol{G}}^T - \tilde{\boldsymbol{N}}_2$$

$$\tilde{\Xi}_{33} = -\tilde{\boldsymbol{X}}_{22} - \tilde{\boldsymbol{X}}_{22}^T - \tilde{\boldsymbol{M}}_3^T - \tilde{\boldsymbol{M}}_3 - \varepsilon_3 \boldsymbol{B}\tilde{\boldsymbol{K}} - \varepsilon_3 \tilde{\boldsymbol{K}}^T \boldsymbol{B}^T$$

$$\tilde{\Xi}_{34} = -\tilde{\boldsymbol{X}}_{23} - \tilde{\boldsymbol{U}}_{12} - \tilde{\boldsymbol{M}}_4^T - \tilde{\boldsymbol{N}}_3 - \varepsilon_4 \tilde{\boldsymbol{K}}^T \boldsymbol{B}^T$$

$$\tilde{\Xi}_{44} = -\tilde{\boldsymbol{X}}_{33} - \frac{1}{d}\tilde{\boldsymbol{U}}_{22} - \tilde{\boldsymbol{N}}_4^T - \tilde{\boldsymbol{N}}_4$$

$$\tilde{\Omega}_{11} = d\left(\tilde{\boldsymbol{X}}_{13} + \tilde{\boldsymbol{X}}_{13}^T\right) + d\tilde{\boldsymbol{U}}_{22} - \tilde{\boldsymbol{Z}}$$

$$\tilde{\Omega}_{12} = d\tilde{\boldsymbol{X}}_{11} + d\tilde{\boldsymbol{X}}_{11}^T$$

$$\tilde{\Omega}_{13} = d\tilde{\boldsymbol{X}}_{23}^T + d\tilde{\boldsymbol{U}}_{12}^T + \tilde{\boldsymbol{Z}}$$

$$\tilde{\Omega}_{22} = d\tilde{\boldsymbol{R}}_{11} + d\tilde{\boldsymbol{Q}} + \frac{d^2}{4}\tilde{\boldsymbol{Z}}$$

$$\tilde{\Omega}_{23} = -d\left(\tilde{\boldsymbol{X}}_{11} + \tilde{\boldsymbol{X}}_{22}\right) + d\tilde{\boldsymbol{R}}_{12}$$

$$\tilde{\Omega}_{33} = d\tilde{\boldsymbol{R}}_{22} + d\tilde{\boldsymbol{U}}_{11} - \tilde{\boldsymbol{Z}}$$

The controller is derived that

$$\boldsymbol{K} = \tilde{\boldsymbol{K}}\tilde{\boldsymbol{G}}^{-T} \tag{25}$$

Proof: Denoting

$$\begin{aligned}
&\tilde{\boldsymbol{G}} = \boldsymbol{G}^{-1}, \tilde{\boldsymbol{K}} = \boldsymbol{K}\tilde{\boldsymbol{G}}^{T}, \tilde{\boldsymbol{P}} = \tilde{\boldsymbol{G}}\boldsymbol{P}\tilde{\boldsymbol{G}}^{T}, \tilde{\boldsymbol{X}}_{11} = \tilde{\boldsymbol{G}}\boldsymbol{X}_{11}\tilde{\boldsymbol{G}}^{T}, \tilde{\boldsymbol{X}}_{22} = \tilde{\boldsymbol{G}}\boldsymbol{X}_{22}\tilde{\boldsymbol{G}}^{T}, \tilde{\boldsymbol{X}}_{13} = \tilde{\boldsymbol{G}}\boldsymbol{X}_{13}\tilde{\boldsymbol{G}}^{T},\\
&\tilde{\boldsymbol{X}}_{23} = \tilde{\boldsymbol{G}}\boldsymbol{X}_{23}\tilde{\boldsymbol{G}}^{T}, \tilde{\boldsymbol{X}}_{33} = \tilde{\boldsymbol{G}}\boldsymbol{X}_{33}\tilde{\boldsymbol{G}}^{T}, \tilde{\boldsymbol{R}}_{11} = \tilde{\boldsymbol{G}}\boldsymbol{R}_{11}\tilde{\boldsymbol{G}}^{T}, \tilde{\boldsymbol{R}}_{12} = \tilde{\boldsymbol{G}}\boldsymbol{R}_{12}\tilde{\boldsymbol{G}}^{T}, \tilde{\boldsymbol{R}}_{22} = \tilde{\boldsymbol{G}}\boldsymbol{R}_{22}\tilde{\boldsymbol{G}}^{T},\\
&\tilde{\boldsymbol{Q}} = \tilde{\boldsymbol{G}}\boldsymbol{Q}\tilde{\boldsymbol{G}}^{T}, \tilde{\boldsymbol{U}}_{11} = \tilde{\boldsymbol{G}}\boldsymbol{U}_{11}\tilde{\boldsymbol{G}}^{T}, \tilde{\boldsymbol{U}}_{12} = \tilde{\boldsymbol{G}}\boldsymbol{U}_{12}\tilde{\boldsymbol{G}}^{T}, \tilde{\boldsymbol{U}}_{22} = \tilde{\boldsymbol{G}}\boldsymbol{U}_{22}\tilde{\boldsymbol{G}}^{T}, \tilde{\boldsymbol{Z}} = \tilde{\boldsymbol{G}}\boldsymbol{Z}\tilde{\boldsymbol{G}}^{T},\\
&\Upsilon_1 = diag\left\{\tilde{\boldsymbol{G}},\tilde{\boldsymbol{G}},\tilde{\boldsymbol{G}}\right\}, \Upsilon_2 = diag\left\{\tilde{\boldsymbol{G}},\tilde{\boldsymbol{G}},\tilde{\boldsymbol{G}},\tilde{\boldsymbol{G}}\right\}, \Upsilon_3 = diag\left\{\tilde{\boldsymbol{G}},\tilde{\boldsymbol{G}},\tilde{\boldsymbol{G}},\tilde{\boldsymbol{G}},\tilde{\boldsymbol{G}},\tilde{\boldsymbol{G}}\right\},\\
&\tilde{\boldsymbol{M}} = \Upsilon_2\boldsymbol{M}\Upsilon_2^{T}, \tilde{\boldsymbol{N}} = \Upsilon_2\boldsymbol{N}\Upsilon_2^{T}.
\end{aligned}$$

Pre- and post-multiplying (9)–(11) by $\Upsilon_1, \Upsilon_2, \Upsilon_3$ and $\Upsilon_1^T, \Upsilon_2^T, \Upsilon_3^T$ respectively, (22)–(24) are obtained. This completed the proof.

5. Numerical examples

In this section, to vertify the performance of the given method, a simulation example for a LC is given [43]. The LC model parameters are considered in Table 1 as follow.

Table 1. LC model parameters.

Items	Symbol	Values
Length between perpendiculars	L_{pp}	220.3 m
Breadth at waterline	B_{wl}	32.2 m
Draft amidships	T_m	7.2 m
Displacement	∇	33,229 t
Vert. location of canter of gravity	KG	15.1 m
Metacentric height	GM	2.75 m
Transverse gyradius	k_{xx}	12.9 m
Longitudinal gyradius	k_{yy}	55.1 m
Vertical gyradius	k_{zz}	55.1 m

And the $\boldsymbol{M}$ and $\boldsymbol{D}$ in model (1) are

$$\boldsymbol{M} = \begin{bmatrix} 0.754 & 0 & 0 \\ 0 & 1.199 & 0.211 \\ 0 & 0.029 & 0.524 \end{bmatrix}, \boldsymbol{D} = \begin{bmatrix} 0.014 & 0 & 0 \\ 0 & 0.102 & -0.0024 \\ 0 & 0.192 & 0.095 \end{bmatrix}$$

Noted that $\boldsymbol{A} = \begin{bmatrix} 0 & \boldsymbol{I} \\ 0 & -\boldsymbol{M}^{-1}\boldsymbol{D} \end{bmatrix}$, $\boldsymbol{B} = \begin{bmatrix} 0 \\ \boldsymbol{M}^{-1} \end{bmatrix}$, $\boldsymbol{B}_w = \begin{bmatrix} 0 \\ \boldsymbol{M}^{-1} \end{bmatrix}$, then

$$A=\begin{bmatrix}0&0&0&1&0&0\\0&0&0&0&1&0\\0&0&0&0&0&1\\0&0&0&-0.0186&0&0\\0&0&0&0&-0.0208&0.0342\\0&0&0&0&-0.3653&-0.1832\end{bmatrix},$$

$$B=B_w=\begin{bmatrix}0&0&0\\0&0&0\\0&0&0\\1.3263&0&0\\0&0.8422&-0.3391\\0&-0.0466&1.9272\end{bmatrix}.$$

First, from Table 2, the maximum sampling period obtained by theorem 2 is $d=0.652$, which improves [37–39] above 160.8, 146.97 and 22.56% respectively. One can find that the controller in this paper can obtain longer sampling period than that in [37–39].

Table 2. Maximum values of the upper sampling period.

Method	[37]	[38]	[39]	Theorem1
d_2	0.25	0.264	0.532	0.652

The initial value of system state is assumed as $x_s(t)=\begin{bmatrix}10&10&0.1&0&0&0\end{bmatrix}$, and $d=3.5513, \varepsilon_1=\varepsilon_2=\varepsilon_3=\varepsilon_4=1,$ The desired value of system state is $x_r(t)=\begin{bmatrix}0&0&0&0&0&0\end{bmatrix}$. Then, the gain can be computed that

$$K=\begin{bmatrix}-9.6426&0&0&-20.1006&0&0\\0&-15.3203&-0.5965&0&-32.0584&-1.4204\\0&1.1998&-5.7224&-0.0022&0.8754&-12.7550\end{bmatrix}.$$

The external environment disturbance is considered that

$$w(t)=\left[\sin(0.3t),\sin(0.2t),\sin(0.1t)\right]$$

Compared the results with the reference [39] which used the normal LKF to deal with the sampled-data issue of the DPS, the simulation results are shown in Figures 5–10 respectively. Figures 5–8 are the responses of the ship's positions and yaw angle. It can be seen that the stable time required to achieve the expected positions and yaw angle using normal LKF in [39] is 20 seconds, while the stable time based on improved LKF in the paper is 12 seconds, which improves the [39] about 40%.

Figures 8–10 are the responses of the velocities. It is shown that the stable time required to achieve the expected velocities using normal LKF in [39] is 22 seconds, while the stable time based on improved LKF in the paper is 15 seconds, which improves the [39] about 31.81%.

From Figures 5–10, we can see that in the presence of external environmental disturbances, the sampled-data controller designed in the paper can track the desired goal of the ship more smoothly and quickly. Besides, the fluctuations of the system are fewer. Therefore, the proposed sampled-data controller is more effective and robustness.

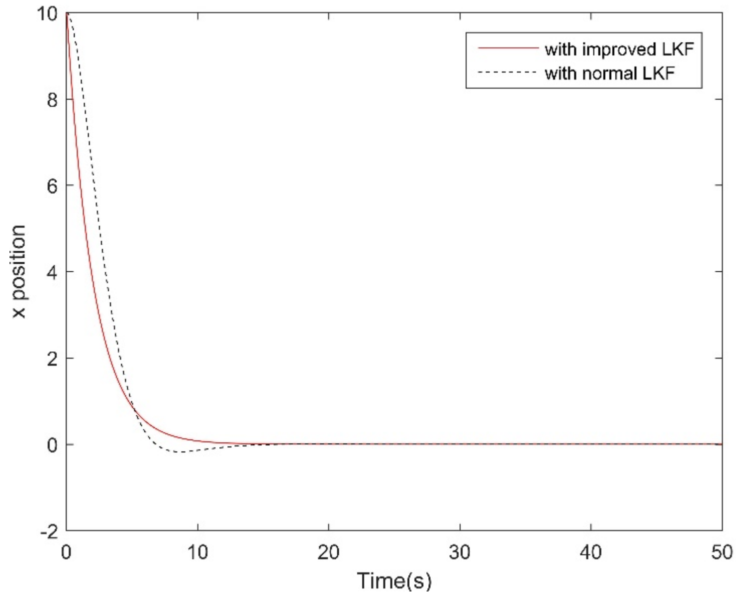

Figure 5. Compared with the x position of the DPS.

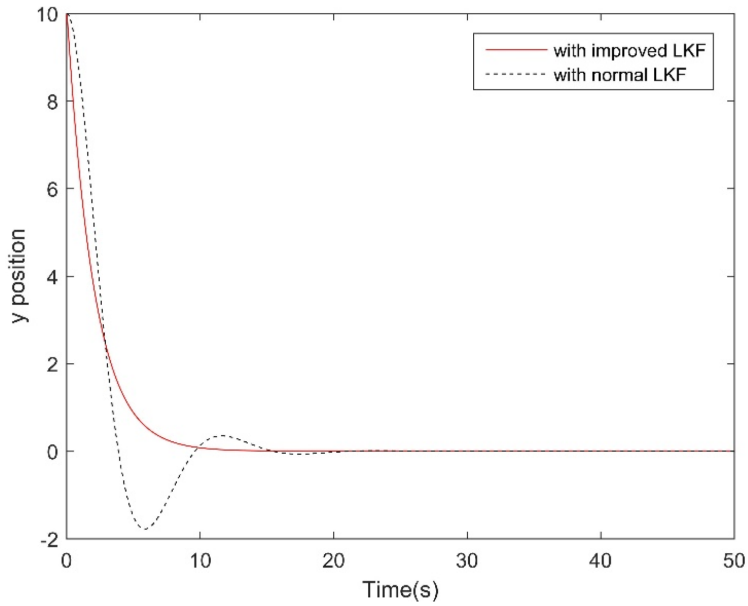

Figure 6. Compared with the y position of the DPS.

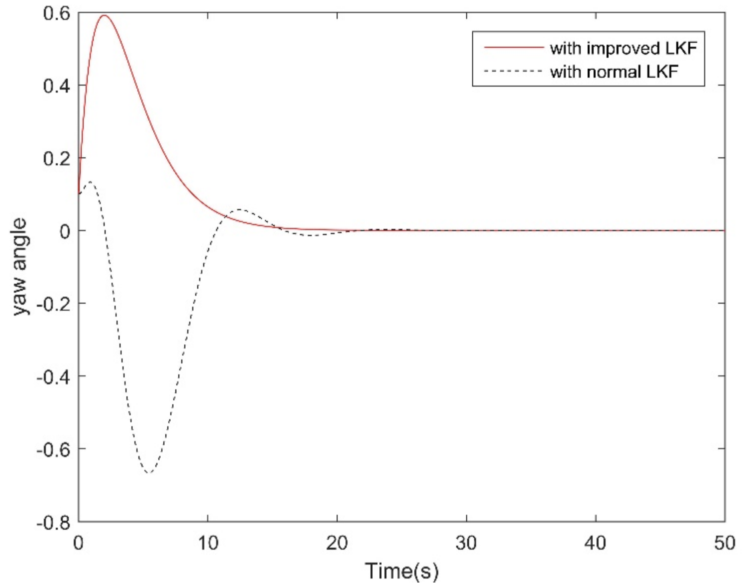

Figure 7. Compared with the yaw angle of the DPS.

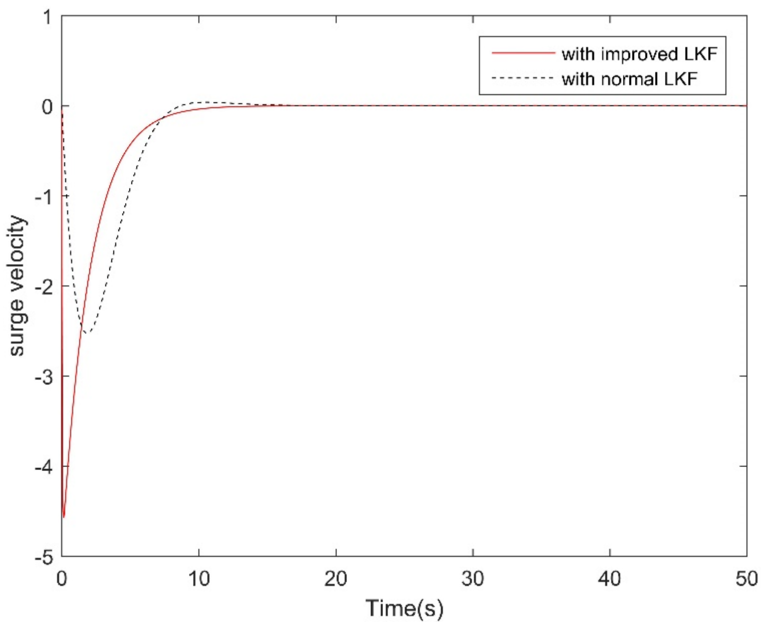

Figure 8. Compared with the surge velocity of the DPS.

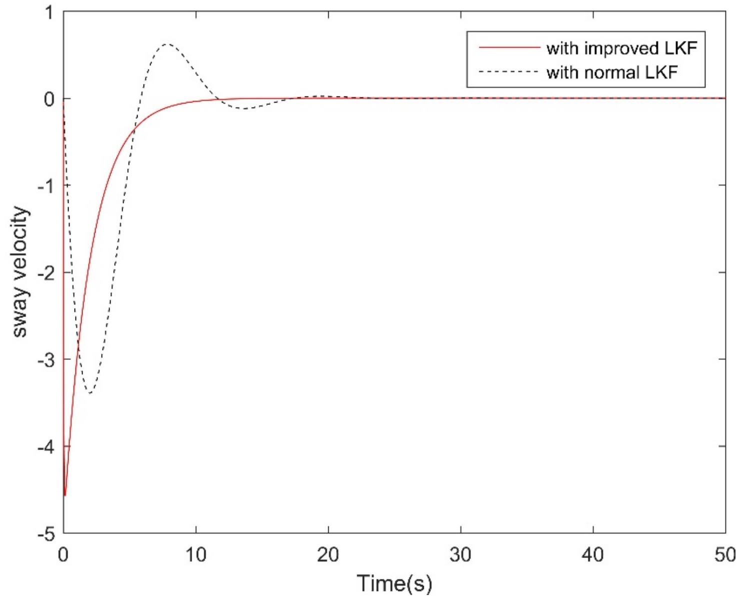

Figure 9. Compared with the sway velocity of the DPS.

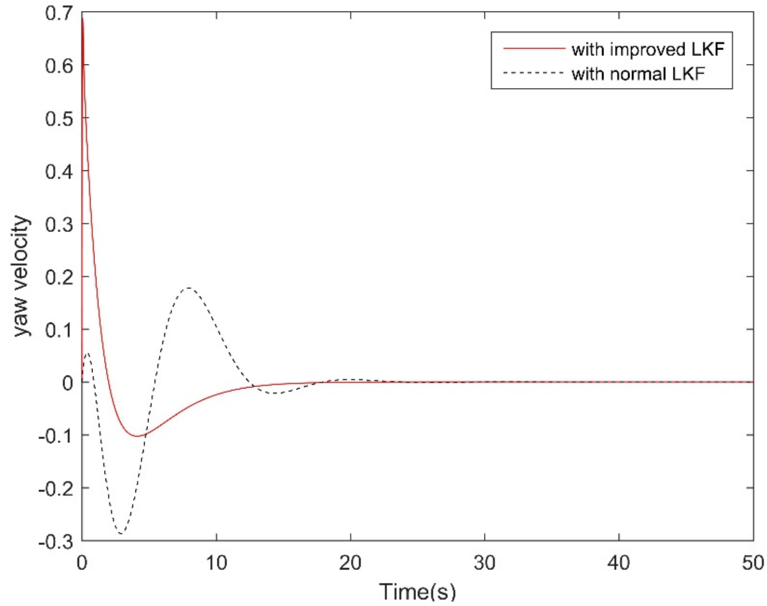

Figure 10. Compared with the yaw velocity of the DPS.

6. Conclusions

This article focused on the sampled-data issue for the LC with DPS. By constructing an improved LKF, the information about sampling modes is fully captured. Then, the conditions of asymptotical stability are present by means of LMI. Additionally, the sampled-data controller for LC with DPS is designed by analyzing the stabilization conditions. A numerical example is provided to illustrate that the proposed methods are effective and less conservativeness can be achieved. It is worth mentioning that the ship motion model only considers the linear problems, which may result in approximate errors in the actual object and reduce the robustness performance. In future research, the nonlinear systems and the modeling errors will be considered in the control synthesis process. In addition, other practical situations such as input saturation and incomplete state information will also be studied.

Use of AI tools declaration

The authors declare they have not used Artificial Intelligence (AI) tools in the creation of this article.

Acknowledgments

This study was funded by Undergraduate Education and Teaching Reform Research Project of Fujian Province in 2022 (FBJG20220194); Graduate Education and Teaching Reform Research project of Jimei University in 2021 (YJG2105); National Natural Science Foundation of China (51879119); Youth Innovation Foundation of Xiamen (3502Z20206019); The Natural Science Foundation of Fujian Province (2021J01822).

Conflict of interest

The authors declare there is no conflict of interest.

References

1. H. R. Karimi, Y. Lu, Guidance and control methodologies for marine vehicles: A survey, *Control Eng. Pract.*, **111** (2021), 104785. https://doi.org/10.1016/j.conengprac.2021.104785
2. H. Liang, L. Li, J. Ou, Coupled control of the horizontal and vertical plane motions of a semi-submersible platform by a dynamic positioning system, *J. Mar. Sci. Technol.*, **20** (2015), 776–786. https://doi.org/10.1007/s00773-015-0322-5
3. M. C. Fang, Z. Y. Lee, Application of neuro-fuzzy algorithm to portable dynamic positioning control system for ships, *Int. J. Nav. Archit. Ocean Eng.*, **8** (2016), 38–52. ttps://doi.org/10.1016/j.ijnaoe.2015.09.003
4. G. Zhang, Y. Cai, W. Zhang, Robust neural control for dynamic positioning ships with the optimum-seeking guidance, *IEEE Trans. Syst. Man Cybern. Syst.*, **47** (2017), 1500–1509. https://doi.org/10.1109/TSMC.2016.2628859
5. W. E. Ngongi, J. Du, R. Wang, Robust fuzzy controller design for dynamic positioning system of ships, *Int. J. Control Autom. Syst.*, **13** (2015), 1294–1305. https://doi.org/10.1007/s12555-014-0239-5
6. J. Li, G. Zhang, Q. Shan, W. Zhang, A novel cooperative design for USV-UAV systems: 3D mapping guidance and adaptive fuzzy control, *IEEE Trans. Control Network Syst.*, **2022** (2022). https://doi.org/10.1109/TCNS.2022.3220705
7. G. Zhang, J. Li, X. Jin, C. Liu, Robust adaptive neural control for wing-sail-assisted vehicle via the multiport event-triggered approach, *IEEE Trans. Cybern.*, **52** (2021), 12916–12928. https://doi.org/10.1109/TCYB.2021.3091580

8. Y. Wang, X. Yang, H. Yan, Reliable fuzzy tracking control of near-space hypersonic vehicle using aperiodic measurement information, *IEEE Trans. Ind. Electron.*, **66** (2019), 9439–9447. https://doi.org/10.1109/TIE.2019.2892696
9. Y. Wei, H. R. Karimi, S. Yang, New results on sampled-data output-feedback control of linear parameter-varying systems, *Int. J. Robust Nonlinear Control*, **32** (2022), 5070–5085. https://doi.org/10.1002/rnc.6099
10. Y. Wang, H. R. Karimi, H. K. Lam, H. Shen, An improved result on exponential stabilization of sampled-data fuzzy systems, *IEEE Trans. Fuzzy Syst.*, **26** (2018), 3875–3883. https://doi.org/10.1109/TFUZZ.2018.2852281
11. D. Zhang, L. Liu, G. Feng, Consensus of heterogeneous linear multiagent systems subject to aperiodic sampled-data and DoS attack, *IEEE Trans. Cybern.*, **49** (2018), 1501–1511. https://doi.org/10.1109/TCYB.2018.2806387
12. X. L. Zhu, B. Chen, D. Yue, Y. Wang, An improved input delay approach to stabilization of fuzzy systems under variable sampling, *IEEE Trans. Fuzzy Syst*., **20** (2012), 330–341. https://doi.org/10.1109/TFUZZ.2011.2174242
13. Y. Wang, Y. Xia, P. Zhou, Fuzzy-model-based sampled-data control of chaotic systems: A fuzzy time-dependent Lyapunov–Krasovskii functional approach, *IEEE Trans. Fuzzy Syst.*, **25** (2016), 1672–1684. https://doi.org/10.1109/TFUZZ.2016.2617378
14. Y. Wang, P. Shi, On master-slave synchronization of Chaotic Lur'e systems using sampled-data control, *IEEE Trans. Circuits Syst. II*, **85** (2016), 981–992. https://doi.org/10.1007/s11071-016-2737-x
15. W. H. Chen, Z. Wang, X. Lu, On sampled-data control for masterslave synchronization of chaotic Lur'e systems, *IEEE Trans. Circuits Syst. II*, **59** (2012), 515–519. https://doi.org/10.1109/TCSII.2012.2204114
16. H. Xiao, Q. Zhu, H. R. Karimi, Stability of stochastic delay switched neural networks with all unstable subsystems: A multiple discretized Lyapunov-Krasovskii functionals method, *Inf. Sci.*, **582** (2022), 302–315. https://doi.org/10.1016/j.ins.2021.09.027
17. Z. G. Wu, P. Shi, H. Su, J. Chu, Stochastic synchronization of Markovian jump neural networks with time-varying delay using sampled data, *IEEE Trans. Cybern.*, **43** (2013), 1796–1806. https://doi.org/10.1109/TSMCB.2012.2230441
18. Z. G. Wu, P. Shi, H. Su, J. Chu, Local synchronization of chaotic neural networks with sampled-data and saturating actuators, *IEEE Trans. Cybern*., **44** (2014), 2635–2645. https://doi.org/10.1109/TCYB.2014.2312004
19. H. R. Karimi, H. Gao. Mixed H2/H∞ output-feedback control of second-order neutral systems with time-varying state and input delays, *ISA Trans.*, **47** (2008), 311–324. https://doi.org/10.1016/j.isatra.2008.04.002
20. F. Ding, T. Chen, Hierarchical identification of lifted state-space models for general dual-rate systems, *IEEE Trans. Circuits Syst. I*, **52** (2005), 1179–1187. https://doi.org/10.1109/TCSI.2005.849144
21. L. Hu, P. Shi, P. Frank, Robust sampled-data control for Markovian jump linear systems, *Automatica*, **42** (2006), 2025–2030. https://doi.org/10.1016/j.automatica.2006.05.029
22. K. Liu, E. Fridman. Wirtinger's inequality and Lyapunov-based sampled-data stabilization, *Automatica*, **48** (2012), 102–108. https://doi.org/10.1016/j.automatica.2011.09.029

23. Z. G. Wu, P. Shi, H. Y. Su, Stochastic synchronization of Markovian jump neural networks with time-varying delay using sampled data, *IEEE Trans. Cybern.*, **43** (2013), 796–1806. https://doi.org/10.1109/TSMCB.2012.2230441
24. E. Yucel, M. S. Ali, N. Gunasekaran, S. Arik, Sampled-data filtering of Takagi-Sugeno fuzzy neural networks with interval time-varying delays, *Fuzzy Sets Syst.*, **316** (2017), 69–81. https://doi.org/10.1016/j.fss.2016.04.014
25. S. Li, L. Yang, K. Li, Z. Gao, Robust sampled-data cruise control scheduling of high speed train, *Transp. Res. Part C*, **46** (2014), 274–283. https://doi.org/10.1016/j.trc.2014.06.004
26. Y. Wang, Q. Wang, P. Zhou, D. Duan, Robust H∞ directional control for a sampled-data autonomous airship, *J. Cent. South Univ.*, **21** (2014),1339–1346. https://doi.org/10.1007/s11771-014-2071-8
27. M. Zheng, Y. Su, S. Yang, L. Li, Reliable fuzzy dynamic positioning tracking controller for unmanned surface vehicles based on aperiodic measurement information, *Int. J. Fuzzy Syst.*, **25** (2023), 358–368. https://doi.org/10.1007/s40815-022-01414-9
28. Z. G. Wu, P. Shi, H. Su, R. Lu, Dissipativity-based sampled-data fuzzy control design and its application to truck-trailer system, *IEEE Tran. Fuzzy Syst.*, **23** (2015), 1669–1679. https://doi.org/10.1109/TFUZZ.2014.2374192
29. C. Qian, H. Du, S. Li, Global stabilization via sampled-data output feedback for a class of linearly uncontrollable and unobservable systems, *IEEE Trans. Autom. Control*, **61** (2016), 4088–4093. https://doi.org/10.1109/TAC.2016.2542238
30. C. Zhang, R. Jia, C. Qian, S. Li, Semi-global stabilization via linear sampled-data output feedback for a class of uncertain nonlinear systems, *Int. J. Robust Nonlinear Control*, **25** (2015), 2041–2061. https://doi.org/10.1002/rnc.3189
31. W. Zou, J. Guo, Z. Xiang, Sampled-data leader-following consensus of second-order non-linear multi-agent systems without velocity measurements, *Int. J. Robust Nonlinear Control*, **28** (2018), 5634–5651. https://doi.org/10.1002/rnc.4340
32. C. Zhang, C. Qian, S. Li, Global decentralized control of interconnected nonlinear systems by sampled-data output feedback, in *Proceedings of 2013 American Control Conference*, (2013), 6559–6564. https://doi.org/10.1109/ACC.2013.6580868
33. F. Yang, H. Zhang, Y. Wang, An enhanced input-delay approach to sampled-data stabilization of T–S fuzzy systems via mixed convex combination, *Nonlinear Dyn.*, **75** (2014), 501–512. https://doi.org/10.1007/s11071-013-1080-8
34. H. Katayama, Nonlinear sampled-data stabilization of dynamically positioned ships, *IEEE Trans. Control Syst. Technol.*, **18** (2010), 463–468. https://doi.org/10.1109/TCST.2009.2014876
35. H. Katayama, H. Aoki, Straight-line trajectory tracking control for sampled-data underactuated ships, *IEEE Trans. Control Syst. Technol.*, **22** (2014), 1638–1645. https://doi.org/10.1109/TCST.2013.2280717
36. M. Zheng, Y. Zhou, S. Yang, L. Li, Robust H∞ control of neutral system for sampled-data dynamic positioning ships, *IMA J. Math. Control Inf.*, **36** (2019), 1325–1345. https://doi.org/10.1093/imamci/dny029
37. S. Yang, M. Zheng, H-infinity fault-tolerant control for dynamic positioning ships based on sampled-data, *J. Control Eng. Appl. Inf.*, **20** (2018), 32–39.
38. M. Zheng, Y. Zhou, S. Yang, Robust fuzzy sampled-data control for dynamic positioning ships, *J. Shanghai Jiaotong Univ.*, **23** (2018), 209–217. https://doi.org/10.1007/s12204-018-1931-z

39. G. Chen, Y. Suo, M. Zheng, S. Yang, L. Li, Reliable tracking control of dynamic positioning ships based on aperiodic measurement information, *J. Control Eng. Appl. Inf.*, **24** (2022), 80–89.
40. J. Sun, G. P. Liu, J. Chen, Delay-dependent stability and stabilization of neutral time-delay systems, *Int. J. Robust Nonlinear Control*, **19** (2009), 1364–1375. https://doi.org/10.1002/rnc.1384
41. H. B. Zeng, Y. He, M. Wu, J. She, Free-matrix-based integral inequality for stability analysis of systems with time-varying delay, *IEEE Trans. Autom. Control*, **60** (2015), 2768–2772. https://doi.org/10.1109/TAC.2015.2404271
42. T. H. Lee, J. H. Park, S. Xu, Relaxed conditions for stability of time-varying delay systems, *Automatica*, **75** (2017), 11–15. https://doi.org/10.1016/j.automatica.2016.08.011
43. P. Valanto, Y. P. Hong, Experimental investigation on ship wave added resistance in regular head, oblique, beam, and following waves, in *The Twenty-fifth International Ocean and Polar Engineering Conference*, 2015.